

Variable Temperature ^{15}N CPMAS NMR Studies of Dye Tautomerism in Crystalline and Amorphous Environments

Bernd Wehrle, Hans-Heinrich Limbach

Institut für Physikalische Chemie der Universität Freiburg i. Br., Albertstraße 21, D-7800 Freiburg, West-Germany

Herbert Zimmermann

Max-Planck-Institut für Medizinische Forschung, Jahnstraße 29, D-6900 Heidelberg, West-Germany

Crystals / Dyes / Glasses / Polymers / Proton Transfer / Spectroscopy, Nuclear Magnetic Resonance

This paper deals with the question of how symmetric double minimum potentials of isolated bistable molecules are affected in the ordered or disordered solid state, in a timescale of slow molecular motion. It is shown that high resolution solid state NMR under conditions of magic angle spinning (MAS) and cross-polarization (CP) can contribute to answering this question. In particular, variable temperature high resolution solid state ^{15}N CPMAS NMR spectra (CP = cross polarization, MAS = magic angle spinning) of ^{15}N enriched tetraaza[14]annulene dyes in the crystalline state and imbedded in disordered glassy polystyrene are presented. These dyes interconvert fast between different tautomeric states whose gasphase degeneracy is lifted in the solid. By contrast to the crystalline state where all dye molecules experience the same solid state perturbation i.e. the same equilibrium constants of tautomerism, molecules dissolved in the glass exist in a multitude of different inequivalent sites with different solid state perturbations. This effect leads to a broad distribution of equilibrium constants of dye tautomerism. This interpretation is confirmed by NMR lineshape simulations and two-dimensional ^{15}N CPMAS NMR experiments by which the temperature dependent distribution can be characterized. High temperature experiments in the region of the glass transition give insights into the process leading to motionally averaged symmetric double minimum potential of tautomerism within the NMR timescale. Thus, solid solution NMR studies provide information about elementary steps of molecular rearrangements in a timescale of slow solvent reorientation. In addition, dyes such as tetraaza[14]annulenes can be used as novel NMR probes for microscopic order and motion in glasses.

1. Introduction

The structure and the dynamics of reactive molecules imbedded in ordered or disordered organic solids are of

considerable interest in physics and chemistry [1–3]. For example, reversible photochemical reactions of dyes in glassy polymers have been proposed for use in optical in-

Ber. Bunsenges. Phys. Chem. 91, 941–950 (1987) – © VCH Verlagsgesellschaft mbH, D-6940 Weinheim, 1987.
0005–9021/87/0909–0941 \$ 02.50/0

Bei den in dieser Zeitschrift wiedergegebenen Gebrauchsnamen, Handelsnamen, Warenbezeichnungen und dgl. handelt es sich häufig um gesetzlich geschützte eingetragene Warenzeichen, auch wenn sie nicht als solche mit ® gekennzeichnet sind.

formation or solar energy storage devices [4–8]. In this context one would like to know more about the question of how molecules break and form chemical bonds when placed in the solid state. Information about such solid effects is needed for modifying kinetic theories of chemical reactions in the gasphase for use in condensed matter. For example, a reduction of the symmetry of a molecule imbedded in a liquid or a solid can influence the reaction mechanism, especially if tunneling is involved, as expected for hydrogen transfer reactions [9,10]. Unfortunately, such solid state effects on chemical reactions are not easy to observe because most reactions require major molecular motions such as translational or rotational diffusion, i.e. processes which are highly restricted in the solid state. Thus, fast reversible solid state reactions which are decoupled in first order from the motion of the matrix molecules are of special interest because of the possibility to study bond breaking and bond formation in or between spatially fixed molecules.

It has been shown that variable temperature (VT) high resolution solid state NMR spectroscopy [11–13] is an excellent method for discovering such reactions [14–22]. In these NMR experiments the chemical shift anisotropy is removed by magic angle spinning (MAS) and dipolar coupling to protons by ^1H decoupling. In addition, the signal to noise ratio is enhanced by crosspolarization (CP) from ^1H to the nucleus studied. In continuation of previous liquid state NMR studies [23–29] we have found by ^{15}N CPMAS NMR spectroscopy that neutral hydrogen transfer reactions between nitrogen atoms in crystalline porphins [17–19], porphycen [19], phthalocyanine [18,20], tetraaza[14]-annulenes [18,21,22] (Figs. 1–5) belong to the class of fast reversible solid state chemical reactions. The mechanism of the porphin tautomerism has been of theoretical interest [23, 27, 32, 33]. Note also that the compounds shown in Figs. 1–5 are dyes which are subject to phototautomerism, even at cryogenic temperatures. This feature has been es-

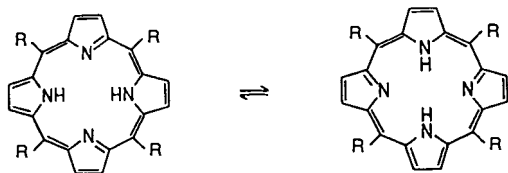


Fig. 1

The tautomerism of porphins. Porphin: $\text{R} = \text{H}$ [19], meso-tetraarylporphin: $\text{R} = \text{Ar}$ [17, 18]

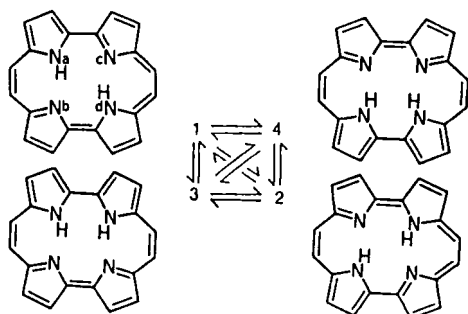


Fig. 2

The tautomerism of porphycen [19]

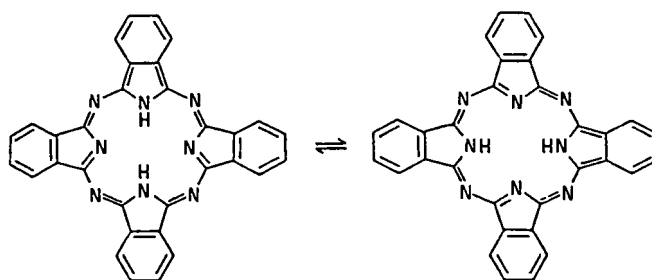


Fig. 3

The tautomerism of phthalocyanine [18,20]

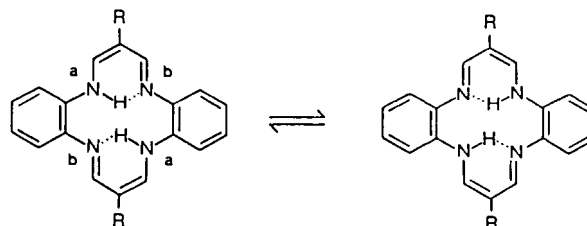


Fig. 4

The tautomerism of dimethyldibenzotetraaza[14]annulene (DTAA) [18, 22, 30], $\text{R} = \text{CH}_3$

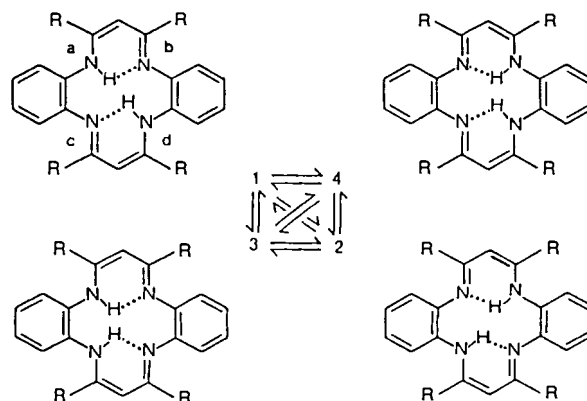


Fig. 5

The tautomerism of tetramethyldibenzotetraaza[14]annulene (TTAA) [21, 31], $\text{R} = \text{CH}_3$

tablished for porphins and phthalocyanines imbedded in organic glasses using laser techniques [4–7]. One major reason why tautomerism in porphines and related compounds is not suppressed in the solid state is that these reactions do not involve ions in contrast to usual proton transfer reactions and that the molecular structure does not allow the breaking of the intramolecular proton transfer network by intermolecular hydrogen bond formation. This does not mean that the gasphase symmetry of the tautomerism is necessarily retained in the solid state. One of the results of our previous ^{15}N CPMAS NMR studies of these systems is indeed that the degeneracy of the tautomers of the reactions shown in Figs. 1 to 5 is lifted more or less in the crystalline state by intermolecular interactions [17–22]. Because of the periodicity of crystals, all reacting molecules of a sample experience the same solid state perturbation.

In this paper we are concerned with the question of how proton tautomerism inside a dye is influenced when the environment is changed from the ordered crystalline to the disordered glassy state. We ask whether the reacting dye molecules experience the structure and the motion of the surrounding matrix molecules. In a theoretical section we first discuss how such effects can be observed by high resolution solid state NMR. After an experimental section we present ^{15}N CPMAS NMR experiments performed on ^{15}N enriched tetraaza[14]annulene dyes, DTAA [30] and TTAA [31] (Figs. 4 and 5) in the crystalline state and of TTAA dissolved in a solid polystyrene glass. Preliminary results have been reported previously for the crystalline compounds [18, 21, 22]. Using the ^{15}N nucleus as spin probe we circumvent the problem of strong ^{13}C matrix signals which has hindered so far the observation of dyes in polymers by ^{13}C CPMAS NMR. As shown below we find that the gasphase degeneracy of tautomers is lifted in the crystalline state; however all molecules are perturbed in the same way. By contrast, in the glassy state we find a broad distribution of dye molecules in different "sites" characterized by different equilibrium constants of fast dye tautomerism. Glass effects on equilibrium constants of fast reversible reactions have not yet been observed to our knowledge. We will be interested in the question of how the different sites interconvert at higher temperatures, leading to a motionally averaged double minimum potential of tautomerism within the NMR timescale.

2. High Resolution NMR Lineshapes of Bistable Molecules in Ordered and Disordered Environments

The NMR lineshape calculations presented in this section were performed with an extended general computer program for exchange broadened NMR spectra [34] based on the density matrix formalism [35]. The program requires as input a complex matrix which depends on the particular exchange problem, and on adjustable parameters such as chemical shifts, populations, rate constants, and linewidths W_0 in the absence of exchange. We discuss here calculated NMR spectra of uncoupled spin 1/2 nuclei S, X etc. of guest molecules which have access to different molecular states and which can exchange between different inequivalent "sites" m, n, \dots characterized by different equilibrium constants

$$K_{mnm} = k_{mnm}/k_{nmm} = x_{nm}/x_{mm} \quad (1)$$

of exchange between the states n and m . k_{mnm} is the corresponding rate constant. x_{mm} is the population of state m in site m , and $x_m = \sum_n x_{nm}$ the population of site m . In addition to the exchange between states we also let the molecules exchange between different sites.

First we treat the case of a bistable molecule in a single site m . Therefore, the subscript m can be omitted. Let the molecule contain two uncoupled spins S and X. In addition, let the molecule be subject to exchange between two states $m = 1$ and $n = 2$. Then Eq. (1) reads

$$K_{12} = k_{12}/k_{21} = x_2/x_1. \quad (2)$$

The calculated exchange broadened NMR spectra of S and X are shown in Fig. 6a. In the slow exchange regime four lines appear at positions given by the chemical shifts of S and X in the two states, i.e. $\nu_{S_1}, \nu_{S_2}, \nu_{X_1}, \nu_{X_2}$. The line intensity

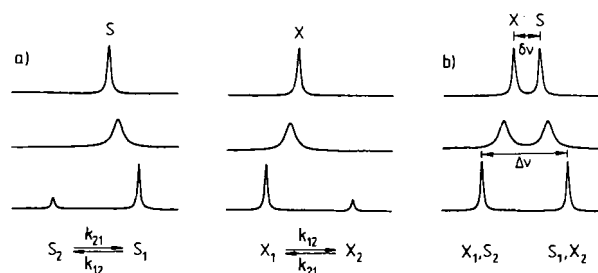


Fig. 6

Calculated spectra for two single spins S and X located in an asymmetric two-state exchange system. The equilibrium constant $K_{12} = k_{12}/k_{21}$ was set to a value of 0.54 in all spectra. The values of k_{12} increase from the bottom to the top. For further explanation see text. a: Spectra calculated for the case that the chemical shifts of all nuclei are different; b: spectra calculated for the case where S and X are in similar chemical environments, i.e. for the case of the validity of Eq. (4)

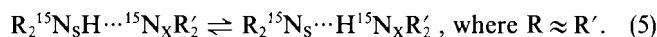
ratios S_2/S_1 and X_2/X_1 correspond to the equilibrium constant K_{12} . As k_{12} is increased the lines broaden and coalesce. The position of the averaged line S is given by

$$\nu_S = x_1 \nu_{S_1} + (1 - x_1) \nu_{S_2}. \quad (3)$$

A similar equation is valid for spin X. Thus, from the line position in the fast exchange the equilibrium constant K_{12} can be obtained if the chemical shifts are known. In Fig. 6b we consider now a special case where

$$\nu_{S_1} = \nu_{X_2} \text{ and } \nu_{S_2} = \nu_{X_1}. \quad (4)$$

This case is typical for proton transfer systems of the type



In the slow exchange regime the spectra then contain only two lines $S = S_1, X_2$ and $X = X_1, S_2$ of equal intensity which broaden and sharpen again as k_{12} is increased. In the fast exchange regime the splitting $\delta\nu = \nu_S - \nu_X$ between the lines S and X is reduced and given by [17, 18]:

$$\delta\nu = \Delta\nu(1 - K_{12})/(1 + K_{12}), \quad (6)$$

where $\Delta\nu = \nu_{S_1} - \nu_{S_2} = \nu_{X_2} - \nu_{X_1}$ is the splitting in the slow exchange regime. For the symmetrical case where $K_{12} = 1$ it follows that $\delta\nu = 0$, i.e. lines S and X coincide.

We consider now the case of a superposition of several discrete sites m, n etc. with different equilibrium constants K_{1m2m} . We restrict our analysis to the special case of very fast state exchange, i.e. the regime where Eq. (3) is valid for the spins in each site. In addition, we assume that Eq. (4) is fulfilled and that the chemical shifts are the same in all sites. Since each site m contains the spins S_m and X_m it contributes two lines to the spectrum with a splitting $\delta\nu_m$ given by

$$\delta\nu_m = \Delta\nu(1 - K_{1m2m})/(1 + K_{1m2m}). \quad (6)$$

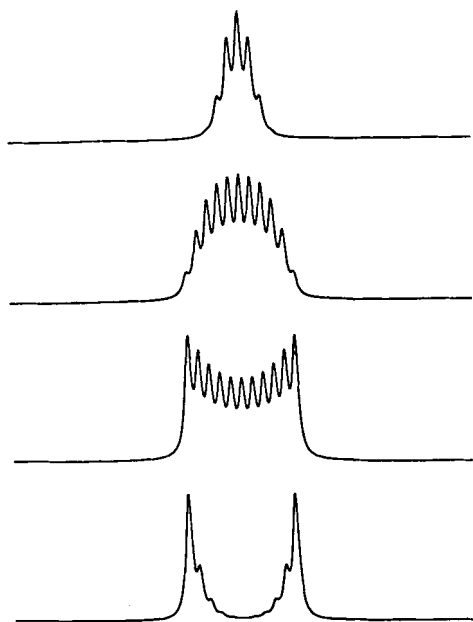


Fig. 7

Calculated NMR spectra for a superposition of doublets S and X with different reduced splittings δv_m due to fast state exchange. Each doublet was generated in a similar way as the top spectrum in Fig. 6b. The different δv_m values correspond to different equilibrium constants of state exchange according to Eq. (6). The doublets were weighed in an arbitrary way. Bottom: large δv_m values i.e. small equilibrium constants dominate; top: small δv_m values i.e. equilibrium constants close to 1 dominate

Fig. 7 shows calculated spectra for a superposition of several discrete sites with different K_{1m2m} i.e. δv_m values, where

$$\delta v_{m+1} = \delta v_m + \Delta f. \quad (7)$$

Δf is a constant frequency increment. The sites are weighed in an arbitrary way. In the spectra at the bottom sites with equilibrium constants $K_{1m2m} \ll 1$ dominate, whereas in the spectra at the top the sites with $K_{1m2m} < 1$ and $K_{1m2m} \approx 1$ are more populated. In principle, the actual distribution can be extracted from the NMR lineshapes. It is, however, sometimes more convenient to introduce a site distribution function in an analytical form which gives the probability ρ of finding a given equilibrium constant. The mostly used distribution function for rate processes in glasses is the so called Williams Watts [36] distribution. Also, a gaussian distribution function of free activation energies has been proposed [3]. We will use in this study a gaussian distribution function of the free reaction enthalpy ΔG_{12} , related to the equilibrium constants K_{12} by the van't Hoff equation

$$K_{12} = \exp(-\Delta G_{12}/RT). \quad (8)$$

R is the gas constant and T the temperature. The distribution is characterized by the width σ and the average value $\overline{\Delta G_{12}}$ of the reaction enthalpy. In fact, the sites in Fig. 7 were weighed using such a distribution function, and only σ and $\overline{\Delta G_{12}}$ were varied. Since only a few sites were considered in Fig. 7 the fine structure of the superposed doublets is still seen. This fine structure disappears when the number of sites

is increased to a degree where the separation between the individual lines becomes smaller than the "individual" or "homogeneous" linewidth W_0 . A further increase of the number of sites does not change the spectra any more. Therefore, for ease of calculation, only a limited number of sites needs to be taken into account. Note, however, that actual parameters extracted using such a discrete site model from experimental spectra have to be extrapolated to an infinite number of sites before they can be interpreted in terms of physical relevant quantities. Finally, it should be mentioned that a spectral line which is constituted by a static superposition of an infinite number of individual sharp lines of different frequency is called "inhomogeneously" broadened [4].

We now allow exchange between the different sites, a process which is not easy to describe. We can imagine two working hypotheses which represent two limits of a complex exchange pattern. In limit (i) each site can exchange with every other site; i.e. the probability of a jump from a site m to a site n is equal to the probability x_n of finding site n . It can be shown that in this case the average lifetime τ_m of all sites between two site exchange processes is the same, i.e. $\tau_m = \tau$. In limit (ii) each site exchanges only with an "adjacent" site and δv changes only in increments Δf , i.e. the equilibrium constants also change only gradually in small increments. In both limits τ can be taken as a measure for the ease of molecular motions which enable the site exchange. We concentrate in this preliminary paper on case (i). Fig. 8 shows the calculated spectral changes in the presence of site exchange according to limit (i). We start at the bottom from an inhomogeneously broadened line, similar to the top spectrum in Fig. 6, where $\tau = \infty$. As we shorten τ , first the homogeneous linewidth of each individual line

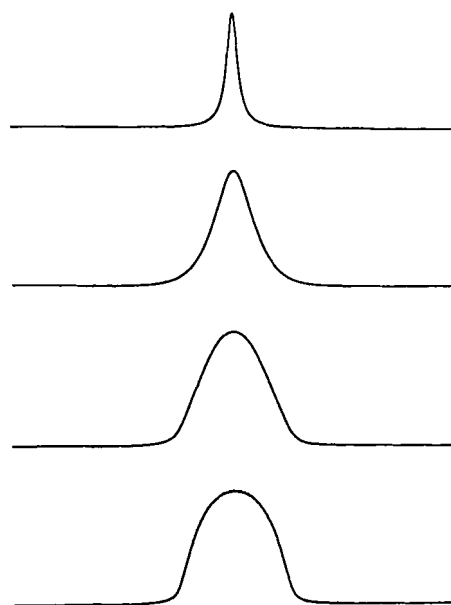


Fig. 8

Effects of a reduced site lifetime τ on the NMR spectra of spins S and X located in different sites characterized by a gaussian distribution of free reaction energies of state exchange. The bottom spectrum where $\tau = \infty$ was generated in a similar way as the spectrum in Fig. 6b, however using 16 instead of 6 sites. From the bottom to the top only the τ values were decreased. Fast site exchange renders all spins S and X equivalent

increases, a fact which cannot be demonstrated in the one-dimensional spectra of Fig. 8, and then all the individual lines coalesce. In the fast site exchange regime only one homogeneously broadened sharp line survives (Fig. 8, top spectrum).

3. Experimental

All NMR experiments were performed on a Bruker CXP 100 pulse FT NMR spectrometer working at 90.02 MHz for protons and at 9.12 MHz for ^{15}N . The spectrometer is equipped with a 2.1 T electromagnet (gap size of 2.2 cm). The CPMAS experiments were performed using a Doty MAS probe [37] adapted for a small magnet gap size. For the longtime stability of the magnetic field a ^2H lock was necessary which was located near the sample. This caused a problem when operating at low temperatures which was solved by using toluene- d_8 as a lock substance. The rotors had an outer diameter of 5 mm, a length of 1 cm, and contained about 50 mg material. Low temperature operation of the magic angle spinner assembly was achieved using cold nitrogen as driving gas. For this purpose a homebuilt heat exchanger was used which has been described previously [20] and which avoids liquefaction of the nitrogen spinning gas when liquid nitrogen is used as cooling medium. ^{15}N enriched DTAA and TTAA were synthesized as described previously by modifying literature procedures [21, 22]. The TTAA/polystyrene samples were prepared as follows. TTAA was dissolved with polystyrene (M.N. = 136000 g mol^{-1} , M.W. = 276000 g mol^{-1}) in chloroform; the solvent was then removed by evacuating the sample for 3 days at 10^{-6} Torr.

4. Results

4.1. ^{15}N CPMAS NMR of Crystalline DTAA

Tetraaza[14]annulenes like DTAA [30] (Fig. 4) are derivatives of malonaldehyde, and it has been an old question whether the H-bonded protons in these compounds move in a double or a single minimum potential [38–40]. High resolution solid state NMR can help to contribute to solving this problem [22]. The ^{15}N CPMAS NMR spectra of DTAA are shown in Fig. 9. The spectra consist of two lines at all temperatures. At low temperature, both the high field line (which we signify as a), characteristic for an NH environment, and the low field line (b), characteristic for an sp^2 nitrogen, are sharp. As the temperature is increased, the lines broaden, sharpen again and move towards each other, but never coalesce. These lineshape changes follow the calculated spectral pattern of Fig. 6b, with $a = \text{S}$ and $b = \text{X}$, where the two interconverting states 1 and 2 can be identified with the two tautomers shown in Fig. 4. The observation of two ^{15}N lines in the fast exchange regime indicates that the degeneracy of the two tautomers 1 and 2 is lifted in the crystalline state. From the ratio $\delta\nu/\Delta\nu$ we find using Eq. (6) that approximately 20% of the minor tautomer 2 is found at room temperature. A reaction enthalpy $\Delta H_{12} = 3.8 \pm 0.4$ kJ mol^{-1} , and a reaction entropy of $\Delta S_{12} = 2 \pm 0.4$ $\text{J K}^{-1} \text{mol}^{-1}$ were obtained [22]. Whereas the entropy difference between the two tautomeric states 1 and 2 found here for crystalline DTAA is negligible, the energy difference is considerable. Unfortunately, a crystal structure of DTAA, which might suggest the reason for this inequivalence, has not yet been obtained. The fact that we find only two ^{15}N lines in the fast exchange regime indicates that the four nitrogen atoms in solid DTAA are pairwise equivalent, i.e. that the two proton transfer units are characterized by the same equilibrium constants (K_{12}) of tautomerism. In other words,

both protons jump in concert or one immediately after the other. The inequivalence of the adjacent nitrogen atoms is also an indication that the molecules do not rotate in the crystalline state. Such a rotation would render all nitrogen atoms equivalent and would result in one sharp averaged ^{15}N line.

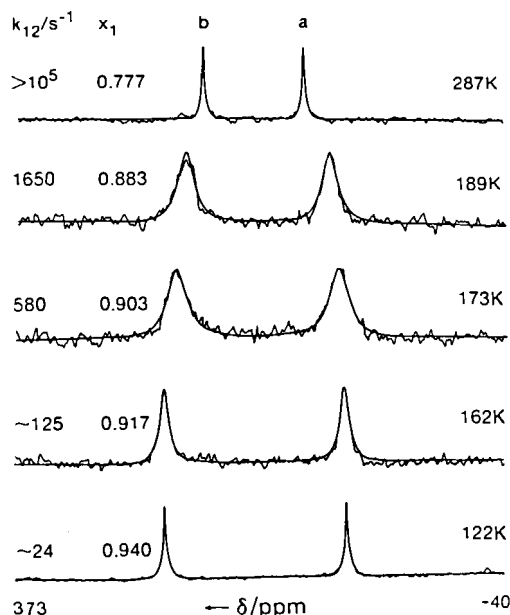


Fig. 9

Superposed experimental and calculated ^{15}N CPMAS NMR spectra of 95% ^{15}N enriched DTAA at 6.082 MHz as a function of temperature. 5 ms cross polarization time, 4 kHz sweep width, 1 s repetition time. Reference: external $^{15}\text{NH}_4\text{NO}_3$. x_1 is the probability of the dominant tautomer, k_{12} the forward rate constant. (Reproduced with permission from Ref. [22])

From the analysis of the lineshapes the forward rate constants $k_{12} \approx 10^7 \exp(-14.7 \text{ kJ mol}^{-1}/RT) \text{ s}^{-1}$ were found. In view of the small temperature range between 160 K and 220 K, over which rate constants could be obtained so far, the temperature dependence of k_{12} given above is preliminary and might be subject to a large error. Deuteration of the molecule in the NH sites resulted in dramatic spectral changes. At 210 K, the deuteron transfer is about 10 times slower than the proton transfer. Thus, we have not only confirmed that the protons in DTAA move in a double minimum potential which is distorted by solid state effects but also that rate constants including kinetic hydrogen/deuterium isotope effects can be associated with this process.

4.2. ^{15}N CPMAS NMR of TTAA in the Crystalline State

The tautomerism in crystalline TTAA [31] (Fig. 5) shows a completely different behavior. Here we observed [21] all possible four tautomers 1 to 4 shown in Fig. 5. These tautomers interconvert very fast on the NMR timescale and are characterized by different energies i.e. different temperature dependent populations. These conclusions can be easily derived from the variable temperature ^{15}N CPMAS NMR spectra of TTAA shown in Figs. 10b and 11b. In the whole temperature region the spectra contain four lines, a–d, of equal intensity whose frequencies are strongly de-

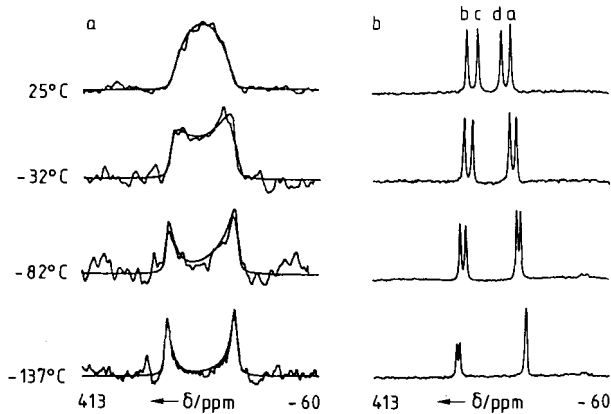


Fig. 10

Low temperature ^{15}N CPMAS NMR spectra of 95% ^{15}N enriched TTAA at 9.12 MHz. a: 9.2% TTAA dissolved in polystyrene; b: crystalline TTAA. The spectra were obtained with a Bruker CXP-100 NMR spectrometer equipped with a Doty [37] probe and a home built low temperature heat exchanger [20]. Experimental conditions: 15 Hz line broadening, 1 K/2 K zero filling, 6 ms cross polarization time, 10000 Hz sweep width, 1.5 s repetition time, $3\ \mu\text{s}$ $^1\text{H}-\pi/2$ pulses, quadrature detection, a: 20000 and b: 500 scans on the average; reference: external $^{15}\text{NH}_4\text{Cl}$. The spectra in Fig. 10a were calculated as described in the text. Parameters of the calculation: $\nu_{\text{N}} = \nu_{\text{S}_2} = \nu_{\text{X}_1} = 2266\ \text{Hz}$ (248.5 ppm), $\nu_{\text{NH}} = \nu_{\text{S}_1} = \nu_{\text{X}_2} = 935\ \text{Hz}$ (102.5 ppm); 20 sites; $\Delta\bar{G}_{12} = 4.3, 4.0, 2.2, 1.1\ \text{kJ mol}^{-1}$ and $\sigma = 1.5, 2.1, 2.4, 2.6\ \text{kJ mol}^{-1}$ at $-137, -82, -32,$ and 25°C ; $\Delta f = 66.5\ \text{Hz}$; $W_0 = 70\ \text{Hz}$

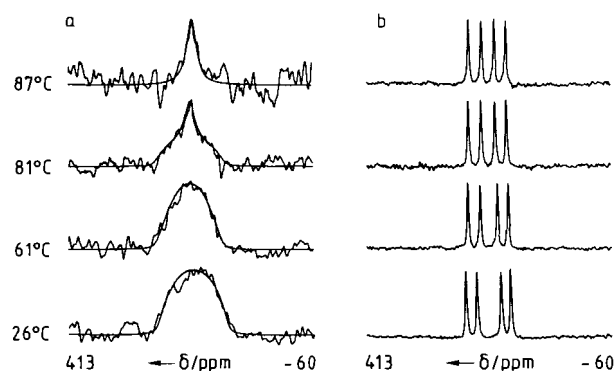


Fig. 11

High temperature ^{15}N CPMAS NMR spectra of 95% ^{15}N enriched TTAA at 9.12 MHz. a: 6% TTAA dissolved in polystyrene; b: crystalline TTAA. For experimental details see Fig. 10. The spectra in Fig. 11a were calculated as described in the text. Parameters of the calculation: 16 sites; $\Delta\bar{G}_{12} = 1.1, 0.5, 0.5, 0.5\ \text{kJ mol}^{-1}$ and $\sigma = 2.6\ \text{kJ mol}^{-1}$ at 26, 61, 81, and 87°C ; $\Delta f = 83.2\ \text{Hz}$; $W_0 = 70\ \text{Hz}$; $\tau^{-1} = 7000$ and $8000\ \text{s}^{-1}$ at 81 and 87°C ; the ratio between the "melted" and the "rigid" signal was 3:7 at 81°C

pendent on temperature. Between 100 K and 80 K, the lowest temperature where experiments were performed, no spectral changes occur [21], indicating that the intrinsic chemical shifts are temperature independent within the experimental error. The overlapping lines a and d were assigned [21] to NH atoms and the two resolved lines b and c to two inequivalent =N- atoms in solid TTAA, as shown in Fig. 5. As the temperature is increased, lines d and c move towards each other without coalescing, as do lines a and b. The low field shift of line a matches the high field shift of

line b. The same is true for lines d and c. Since the intrinsic chemical shifts are temperature independent, these changes can only be explained by fast proton transfer from atom a to b and from atom d to c. In other words, the position of line i depends on the average proton density p_i on atom i. The temperature dependent splitting $\delta\nu_{ab}$ and $\delta\nu_{dc}$ can, therefore, be explained in terms of fast exchange, i.e. with the validity of Eq. (6). Thus, the apparent equilibrium constants K_{ab} and K_{dc} are different in the two $^{15}\text{NH}\cdots^{15}\text{N}$ subunits of TTAA. Two-dimensional exchange experiments [21] revealed the existence of spin diffusion between all lines, arising from dipolar interactions between the nuclei a to d, which was taken as proof that each TTAA molecule contains all four chemically inequivalent nuclei a to d. Thus, since $K_{ab} \neq K_{dc}$, the transfer of the two protons in TTAA must be uncorrelated. These ratios can be related to the equilibrium constants K_{mn} in the following way [21], where $m, n = 1-4$ are the tautomeric states shown in Scheme 5:

$$K_{ab} = K_{14}(1 + K_{42})/(1 + K_{13}), \quad (9)$$

$$K_{dc} = K_{13}(1 + K_{32})/(1 + K_{14}).$$

If the two proton transfer systems ab and dc are independent of each other, i.e. if

$$K_{14} \approx K_{32} \quad \text{and} \quad K_{13} \approx K_{42} \quad (10)$$

is follows that

$$K_{ab} \approx K_{14} \quad \text{and} \quad K_{dc} \approx K_{13}. \quad (11)$$

The different behavior of DTAA and TTAA might be correlated to a steric effect which hinders the coplanar arrangement of the two H-chelate subunits in TTAA [21, 41].

4.3. ^{15}N CPMAS NMR of TTAA in Solid Polystyrene Solution

We come now to the question of how the tautomerism in a dye such as TTAA is affected when the environment is changed from the crystalline state to a solid solution in a disordered matrix such as glassy polystyrene. In order to avoid complications arising from several linebroadening mechanisms we performed solid solution NMR experiments only on TTAA. In this compound the proton transfer is so fast that dynamic linebroadening is absent in contrast to DTAA (see Fig. 9). The experimental and calculated ^{15}N CPMAS NMR spectra of TTAA, dissolved at concentrations of 9.2% and 6% p.w. in glassy polystyrene are shown in Figs. 10 and 11 together with the corresponding crystal spectra. In the disordered solid solution the sharp four lines characteristic for the ordered environment are replaced at room temperature by a broad temperature dependent line which separates into two lines as the sample is cooled. Lowering the TTAA concentration to 2% did not affect the lineshapes; however, in the spectra of the 9.2% sample the four sharp lines of Fig. 10b appeared after several temperature cycles due to slow formation of TTAA microcrystallites which can, thus, be easily distinguished from the dissolved TTAA molecules. Depending on the conditions of

sample preparation an impurity was formed giving rise to the small line at 290 ppm in Fig. 10a. A two-dimensional exchange experiment [15] on a 8% TTAA/polystyrene sample revealed a narrow ridge along the diagonal axis as shown in Fig. 12. This observation proves that the spectra of TTAA in polystyrene are inhomogeneously broadened, i.e. that they are composed of many sharp lines. If the linebroadening were homogeneous, i.e. arising from dynamic processes the two-dimensional signal would extend in all directions [15]. In view of the poor signal to noise ratio no attempt was made to detect possible cross peaks which could arise from spin diffusion [21].

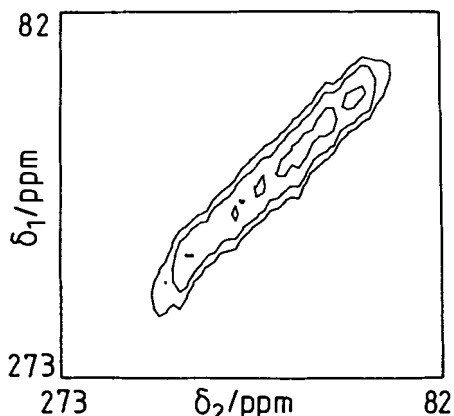


Fig. 12

Two-dimensional magnetization transfer 9.12 MHz ^{15}N CPMAS spectrum (contour plot) at 300 K of a 8.2% solution of TTAA- $^{15}\text{N}_4$ in polystyrene using a mixing time of 1 s. There were 32 by 256 points in the original data matrix, 2048 scans per spectrum. 6 ms cross polarization time, 3 μs $1\text{H}-\pi/2$ pulses, 2.7 s repetition time. Reference: external $^{15}\text{NH}_4\text{Cl}$

The inhomogeneous linebroadening can be explained in terms of the ideas outlined in section 2 by the presence of a broad distribution of sites characterized by different equilibrium constants of tautomerism. In each site m a TTAA molecule is characterized by a certain set of equilibrium constants K_{mnm} , $m, n = 1-4$. For simplification of the lineshape calculations it is useful to assume that both proton transfer systems are independent from each other, i.e. that Eq. (11) is valid. Thus, only single proton transfer systems need to be considered, as in section 2, where each system exists in two tautomeric states 1 and 2, characterized by different equilibrium constants $K_{1,2m}$ in the different sites. The spectra shown in Fig. 10a were then calculated as follows. In view of small individual linewidths as indicated by the two-dimensional exchange experiment in Fig. 12 the inverse site lifetimes τ^{-1} were set to zero. By simulation we find an individual linewidth of $W_0 \approx 70$ Hz which compares well with the value of $W_0 \approx 50$ Hz for the lines in Fig. 10b. W_0 is the sum of the residual inhomogeneous linewidth arising from magic angle misadjustments, magnetic field inhomogeneity, artificial linebroadening etc. and the homogeneous linewidth arising from all possible dynamic processes. The intrinsic chemical shifts of the NH and the =N- atoms were taken as temperature independent. A correction for the different intrinsic line intensities of the NH and the N atoms was introduced taking into account the different cross po-

larization dynamics of these atoms. Additional parameters of the calculations are indicated in Fig. 10. The agreement between the experimental and the calculated lineshapes shown in Fig. 10a is satisfactory and supports our lineshape model. Thus, at room temperature rotational diffusion of TTAA and exchange between different sites are slow on the NMR timescale. These processes would increase the homogeneous linewidth and lead eventually to a collapse of the broad lines in Fig. 10a into one sharp line as proposed in Fig. 8. We find further that ΔG_{12} – although relatively small – decreases slightly with temperature as the average equilibrium constant of tautomerism increases because of the population of higher energy levels. The width of the distribution seems to be fairly constant.

However, what happens when the molecular motions become faster at higher temperatures? The answer is shown in Fig. 11a. In contrast to the prediction of Fig. 8 we do not observe a smooth increase of the site exchange rates with temperature. Major lineshape changes occur only above 75°C when the glass transition region is reached. Above this temperature, a relatively sharp center line appears superimposed on the broad line indicating that a fraction of the dye molecules has become very mobile whereas the other fraction is still immobile. As temperature is further increased the fraction of the mobile dye molecules increases. Above 90°C all dye molecules have become mobile. The NMR lineshapes were calculated as a static superposition of lineshapes arising from exchanging and non exchanging molecules; it was assumed for the mobile molecules that the parameters describing the width and the maximum of the site distribution are the same for the molecules in the mobile and the immobile phase. Values for the site exchange time of the dyes in the mobile phase were extracted from the spectra as indicated in Fig. 11. In view of the assumptions inherent in the calculation we do not, however, stress the physical significance of these preliminary values at present.

5. Discussion

Our results show that ^{15}N CPMAS NMR of ^{15}N enriched molecules in crystalline environments or imbedded in organic glasses such as polystyrene can give not only interesting insights into the dynamics of exchange processes between different molecular states such as tautomerism but also into the way of how these exchange processes are perturbed by the structure and the dynamics of the environment.

For crystalline DTAA we have established a correlated motion of the two protons between two tautomeric states as shown in Fig. 4. This correlation does not necessarily mean that the transfer is concerted but that if the jump of one proton along the intramolecular hydrogen bond is successful the same will be true for the second proton. Thus, diagonal opposite nitrogen atoms experience the same average proton density. This is not the case for crystalline TTAA where all nitrogen atoms experience a different average proton density indicating that all four possible tautomers are present as proposed in Fig. 5. Whereas the double proton transfer in crystalline DTAA was so slow that rate constants of this process and kinetic isotope effects could be

obtained, the tautomerism in TTAA is extremely rapid with respect to the NMR timescale even at very low temperatures. Our working hypothesis as to why the proton transfer in DTAA is much slower than in TTAA is that the degree of coupling of the proton motion in both compounds is different. Independent support for this idea comes from the observation that tetraaza[14]annulenes such as DTAA are dark red due to an electronic absorption band in the 450 nm region [42, 43]. This band is absent in the yellow TTAA [42], which correlates with the fact that the four methyl groups of TTAA sterically hinder a coplanar arrangement of the two chelate subunits in the crystal [41]. Thus, the two H-chelate subunits on TTAA are, to a crude approximation, decoupled electronically leading to independent proton motion, in contrast to DTAA. The question whether tunneling might contribute to the observed rate constants of tautomerism in DTAA might be discussed if the kinetic isotope effects of this reaction had been measured in a wider temperature range.

Nevertheless, there are two common features in the DTAA and the TTAA tautomerism. For both compounds the gasphase degeneracy of equivalent tautomeric states is lifted in the crystalline state. The situation is illustrated in a general way schematically in Fig. 13. Consider a bistable molecule in the gasphase characterized by a symmetric double minimum potential. The reaction entropy ΔS and the reaction energy ΔE between the two states, corresponding to the two potential wells, vanish. Assuming that the reaction is not suppressed in the crystalline state, the gasphase degeneracy will be lifted in the solid if the reacting molecules are placed in a nonsymmetric way with respect to an existing preferential axis. In the first approximation, we assume that ΔS is still close to zero and that the double minimum potential of one molecule will be independent of the molecular state of the neighbouring molecules. In an ordered environment such as a crystal lattice all molecules will then be characterized by the same energy difference $\Delta E \neq 0$ between the two wells of the double minimum potential. The ^{15}N CPMAS NMR experiments presented here and previously [17–22] show that the molecular model expressed in Fig. 13 is realized for the tautomeric reactions of Figs. 1 to 5 within the margin of error of these experiments: e.g., we find values of $\Delta S \approx 0$ but $\Delta E \neq 0$. ΔE depends in a sensitive way on the intermolecular interactions.

The tautomerism of an ensemble of dye molecules such as TTAA imbedded in a disordered glass differs in a characteristic way from the equivalent process in the crystalline state. This conclusion arises from the observation of completely different temperature dependent ^{15}N NMR lineshapes for crystalline TTAA and for TTAA dissolved in polystyrene (Figs. 10–12). These lineshapes are well understood in terms of a multitude of different dye environments or sites with different free reaction energies ΔG of tautomerism. The latter are approximately equal to the energy differences ΔE between the tautomeric states. The NMR spectra could be simulated assuming a Gaussian distribution of ΔG , i.e. ΔE values. The spectra also tell that the proton transfer in TTAA is extremely fast, not only in the sites characterized by a quasisymmetric double minimum potential but also in the sites where the TTAA molecules

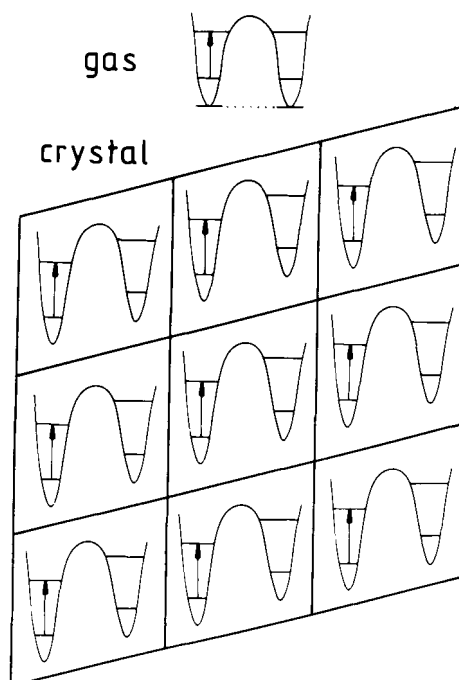


Fig. 13
Perturbation of a symmetric gasphase double minimum potential in the ordered solid state by intermolecular interactions. The arrows indicate the manifold of molecular vibrations

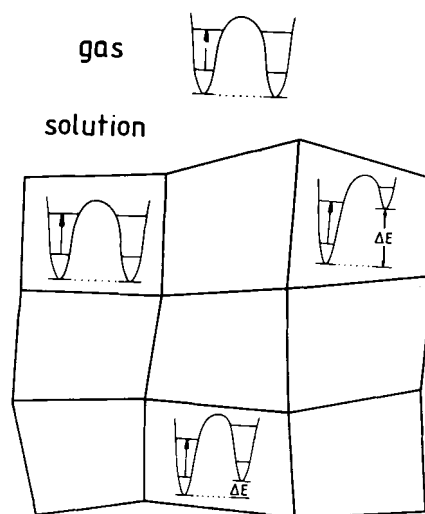


Fig. 14
Perturbation of a symmetric gasphase double minimum potential in the disordered solid state by intermolecular interactions. The arrows indicate the manifold of molecular vibrations

experience large perturbations of the double minimum potential of tautomerism. Because of this fast proton transfer we studied, in fact, glassy solutions of TTAA and not of DTAA; we thus avoided complications arising from dynamic linebroadening due to slow proton transfer present in solid DTAA (see Fig. 9). It can, however, be anticipated, that this more complicated case can be handled better by performing two-dimensional NMR studies such as shown in Fig. 12.

From these results a molecular model arises, shown in Fig. 14, of how a symmetric double minimum potential of an isolated bistable molecule in the gasphase is perturbed by intermolecular interactions when the molecule is imbedded in disordered condensed media such as a glass. In this environment the periodicity of the unit cells in which the bistable molecule is located has been lost as is indicated schematically in Fig. 14. Depending on the environment the double minimum potential is distorted in a different way leading to a continuous distribution of ΔE values of tautomerism. The model represents in a way a snapshot of reacting molecules in disordered condensed matter, in a timescale of slow molecular motion, i.e. it might not only be applied to glasses but also to liquids, although, in a much shorter timescale, as realized, for example, in IR spectroscopy. Thus, results of both NMR and IR experiments on glassy solutions may directly be compared because both methods see the observed molecules as immobile. In particular, the question could be studied whether vibrational transitions, indicated schematically by arrows in Figs. 13 and 14, which are strongly coupled to the reaction coordinate of the proton motion — established by NMR — are inhomogeneously broadened in disordered solutions as compared to the gasphase or the crystalline state.

The last question we have to address is the process of motional averaging of the different asymmetric double minimum potentials in the different sites into one effective symmetric double minimum potential within the NMR timescale. This process is treated here as exchange between different sites and was observed experimentally in the temperature region where the glass transition of TTAA occurs, i.e. in a region where the molecular motion of the matrix molecules becomes fast (Fig. 11a). Surprisingly, we find a static superposition of "melted" regions with a short lifetime of site exchange of the dye molecules and of "rigid" regions where the dye molecules are stuck. In other words, the system cannot be described by a single site exchange lifetime τ , but at least two, and possibly a distribution of lifetimes τ are needed for proper description. The fraction of the melted region increases rapidly as temperature is increased above the glass temperature. A similar separation in two phases, one characterized by long, and the other by short correlation times of molecular motions has been found previously by NMR for organic glasses [16, 44].

We conclude that information on fast chemical reactions under conditions of slow solvent reorientation can be obtained by solid solution state NMR. When analyzing exchange broadened NMR spectra of molecules in the disordered solid state, inhomogeneous linebroadening arising from glass effects on equilibrium constants has to be taken into account in addition to glass effects on molecular dynamics. We propose to use this effect for probing local order and motion in glasses by NMR. Interesting insights might be obtained if optical and NMR studies of the same system can be combined. Further work is underway in order to examine the effects of solute-solvent interactions, motion, and chemical kinetics on the ^{15}N CPMAS NMR spectra of dyes in solid solutions.

We thank Dr. C. S. Yannoni and R. D. Kendrick, IBM Almaden Research Laboratory, San Jose, USA, for stimulating discussions

and for their contributions to this work. We also thank the Deutsche Forschungsgemeinschaft, Bonn-Bad Godesberg, the Stiftung Volkswagenwerk, Hannover, and the Fonds der Chemischen Industrie, Frankfurt, for financial support.

References

- [1] S. R. Elliott, C. N. R. Rao, and J. M. Thomas, *Angew. Chem.* **98**, 31 (1986); *Angew. Chem. Int. Ed.* **25**, 31 (1986).
- [2] W. Siebrand and T. A. Wildman, *Acc. Chem. Res.* **19**, 238 (1986).
- [3] W. J. Albery, P. N. Bartlett, C. P. Wilde, and J. R. Darwent, *J. Am. Chem. Soc.* **107**, 1854 (1985).
- [4] J. Friedrich and D. Haarer, *Angew. Chem.* **96**, 96 (1984); *Angew. Chem. Int. Ed.* **23**, 113 (1984).
- [5] S. Völker and J. H. van der Waals, *Mol. Phys.* **32**, 1703 (1976).
- [6] S. Völker and R. Macfarlane, *IBM Res. Develop.* **23**, 547 (1979).
- [7] W. E. Moerner, *J. Mol. Electronics* **1**, 55 (1986).
- [8] G. Kämpff, *Ber. Bunsenges. Phys. Chem.* **89**, 1179 (1985).
- [9] J. Brickmann and H. Zimmermann, *Ber. Bunsenges. Phys. Chem.* **70**, 157 (1966); *ibid.* **70**, 521 (1966); *ibid.* **71**, 160 (1971); J. Brickmann and H. Zimmermann, *J. Chem. Phys.* **50**, 1608 (1969); J. Brickmann, *Ber. Bunsenges. Phys. Chem.* **84**, 186 (1980); M. Klöffler and J. Brickmann, *Ber. Bunsenges. Phys. Chem.* **86**, 203 (1982).
- [10] R. P. Bell, *The Tunnel Effect in Chemistry*, Chapman and Hall, London 1980.
- [11] J. Schaefer and E. O. Stejskal, *J. Am. Chem. Soc.* **98**, 1031 (1976).
- [12] J. R. Lyerla, C. S. Yannoni, and C. A. Fyfe, *Acc. Chem. Res.* **15**, 208 (1982).
- [13] C. A. Fyfe, *Solid State NMR for Chemists*, C. F. C. Press, Guelph, Ontario 1983.
- [14] N. M. Szeverenyi, A. Bax, and G. E. Maciel, *J. Am. Chem. Soc.* **105**, 2579 (1983).
- [15] N. M. Szeverenyi, M. J. Sullivan, and G. E. Maciel, *J. Magn. Reson.* **47**, 462 (1982).
- [16] P. C. Myrre, J. D. Kruger, B. L. Hammond, S. M. Lok, C. S. Yannoni, V. Macho, H. H. Limbach, and H. M. Vieth, *J. Am. Chem. Soc.* **106**, 6079 (1984).
- [17] H. H. Limbach, J. Hennig, R. D. Kendrick, and C. S. Yannoni, *J. Am. Chem. Soc.* **106**, 4059 (1984).
- [18] H. H. Limbach, D. Gerritzen, H. Rumpel, B. Wehrle, G. Otting, H. Zimmermann, R. D. Kendrick, and C. S. Yannoni, in: "Photoreaktive Festkörper", p. 19, eds. H. Sixl, J. Friedrich, and C. Bräuchle, Karlsruhe 1985.
- [19] B. Wehrle, H. H. Limbach, M. Köcher, and E. Vogel, *Angew. Chemie*, in press.
- [20] R. D. Kendrick, S. Friedrich, B. Wehrle, H. H. Limbach, and C. S. Yannoni, *J. Magn. Reson.* **65**, 159 (1985).
- [21] H. H. Limbach, B. Wehrle, H. Zimmermann, R. D. Kendrick, and C. S. Yannoni, *J. Am. Chem. Soc.* **109**, 929 (1987).
- [22] H. H. Limbach, B. Wehrle, H. Zimmermann, R. D. Kendrick, and C. S. Yannoni, *Angew. Chem.* **99**, 241 (1987); *Angew. Chem. Int. Ed.* **26**, 247 (1987).
- [23] H. H. Limbach, J. Hennig, D. Gerritzen, and H. Rumpel, *Faraday Discuss. Chem. Soc.* **74**, 822 (1982).
- [24] D. Gerritzen and H. H. Limbach, *Ber. Bunsenges. Phys. Chem.* **85**, 527 (1981).
- [25] J. Hennig and H. H. Limbach, *J. Am. Chem. Soc.* **106**, 292 (1984).
- [26] D. Gerritzen and H. H. Limbach, *J. Am. Chem. Soc.* **106**, 869 (1984).
- [27] H. H. Limbach, J. Hennig, and J. Stulz, *J. Chem. Phys.* **78**, 5432 (1983); H. H. Limbach, *J. Chem. Phys.* **80**, 5343 (1984).
- [28] M. Schlabach, B. Wehrle, H. H. Limbach, E. Bunnenberg, A. Knieringer, A. Y. L. Shu, B. R. Tolf, and C. Djerassi, *J. Am. Chem. Soc.* **108**, 3856 (1986).
- [29] G. Otting, H. Rumpel, L. Meschede, G. Scherer, and H. H. Limbach, *Ber. Bunsenges. Phys. Chem.* **90**, 1122 (1986).
- [30] DTAA \equiv 1,8-dihydro-6,13-dimethyldibenzo(b,i)- $^{15}\text{N}_4$ -(1,4,8,11)-tetraazacyclotetradeca-4,6,11,13-tetraen (dimethyldibenzotetraaza[14]annulene).

- [31] TTAA \equiv 1,8-dihydro-5,7,12,14-tetramethyldibenzo(b,i)- $^{15}\text{N}_4$ -(1,4,8,11)-tetraazacyclotetradeca-4,6,11,13-tetraene (tetramethyldibenzotetraaza[14]annulene).
- [32] A. Sarai, *J. Chem. Phys.* **76**, 5554 (1982); *ibid.* **80**, 5431 (1984); G. I. Bersuker and V. Z. Polinger, *Chem. Phys.* **86**, 57 (1984).
- [33] W. Siebrand, T. A. Wildman, and M. Z. Zgierski, *J. Am. Chem. Soc.* **106**, 57 (1984); *ibid.* **106**, 4089 (1984).
- [34] H. H. Limbach, *J. Magn. Reson.* **36**, 287 (1979).
- [35] G. Binsch, *J. Am. Chem. Soc.* **91**, 1304 (1969).
- [36] G. Williams and D. C. Watts, *Trans. Faraday Soc.* **66**, 80 (1970).
- [37] P. D. Ellis and F. D. Doty, *Rev. Sci. Instrum.* **52**, 1868 (1981).
- [38] B. Bock, K. Flatau, H. Junge, M. Kuhr, and H. Musso, *Angew. Chem.* **83**, 239 (1971); *Angew. Chem. Int. Ed.* **83**, 2251 (1971).
- [39] H. H. Limbach and W. Seiffert, *Ber. Bunsenges. Phys. Chem.* **78**, 532 (1974); *ibid.* **78**, 641 (1974).
- [40] S. L. Baugham, R. W. Duerst, W. F. Rowe, Z. Smith, and E. B. Wilson, *J. Am. Chem. Soc.* **103**, 6296 (1981).
- [41] V. L. Goedken, J. J. Pluth, S. M. Peng, and B. Bursten, *J. Am. Chem. Soc.* **98**, 8014 (1976).
- [42] F. A. L'Eplattenier and A. Pugin, *Helv. Chim. Acta* **58**, 917 (1975).
- [43] H. Hiller, P. Dimroth, and H. Pfitzer, *Liebigs Ann. Chem.* **717**, 137 (1968).
- [44] A. D. English and P. Zoller, *Anal. Chim. Acta* **198**, 135 (1986).

Presented at the Discussion Meeting of the Deutsche Bunsen-Gesellschaft für Physikalische Chemie "Physics and Chemistry of Unconventional Organic Materials", Wiesbaden-Naurod, April 29th to May 1st, 1987

E 6559